Molecular Structures of the S124A, S124T, and S124V Site-Directed Mutants of UDP-galactose 4-Epimerase from *Escherichia coli*[†,‡]

James B. Thoden, Andrew M. Gulick, and Hazel M. Holden*

Institute for Enzyme Research, Graduate School, and Department of Biochemistry, University of Wisconsin, Madison, Wisconsin 53705

Received February 25, 1997; Revised Manuscript Received June 17, 1997[⊗]

ABSTRACT: UDP-galactose 4-epimerase plays a critical role in sugar metabolism by catalyzing the interconversion of UDP-galactose and UDP-glucose. Originally, it was assumed that the enzyme contained a "traditional" catalytic base that served to abstract a proton from the 4′-hydroxyl group of the UDP-glucose or UDP-galactose substrates during the course of the reaction. However, recent high-resolution X-ray crystallographic analyses of the protein from *Escherichia coli* have demonstrated the lack of an aspartate, a glutamate, or a histidine residue properly oriented within the active site cleft for serving such a functional role. Rather, the X-ray crystallographic investigation of the epimerase·NADH·UDP-glucose abortive complex from this laboratory has shown that both Ser 124 and Tyr 149 are located within hydrogen bonding distance to the 4′- and 3′-hydroxyl groups of the sugar, respectively. To test the structural role of Ser 124 in the reaction mechanism of epimerase, three site-directed mutant proteins, namely S124A, S124T, and S124V, were constructed and crystals of the S124A·NADH·UDP, S124A·NADH·UDP-glucose, S124T·NADH·UDP-glucose, and S124V·NADH·UDP-glucose complexes were grown. All of the crystals employed in this investigation belonged to the space group $P3_221$ with the following unit cell dimensions: $a = b = 83.8$ Å, $c = 108.4$ Å, and one subunit per asymmetric unit. X-ray data sets were collected to at least 2.15 Å resolution, and each protein model was subsequently refined to an *R* value of lower than 19.0% for all measured X-ray data. The investigations described here demonstrate that the decreases in enzymatic activities observed for these mutant proteins are due to the loss of a properly positioned hydroxyl group at position 124 and not to major tertiary and quaternary structural perturbations. In addition, these structures demonstrate the importance of a hydroxyl group at position 124 in stabilizing the *anti* conformation of the nicotinamide ring as observed in the previous structural analysis of the epimerase·NADH·UDP complex.

UDP-galactose 4-epimerase, hereafter referred to as epimerase, plays a key role in the Leloir pathway for galactose metabolism by catalyzing the interconversion of UDP-galactose and UDP-glucose. Within recent years, epimerase has been the focus of intensive biochemical, structural, and mechanistic investigations. As isolated from *Escherichia coli*, the enzyme is a homodimer with each subunit containing 338 amino acid residues and one tightly bound nicotinamide adenine dinucleotide (*1*, *2*). High-resolution X-ray crystallographic analyses of the enzyme from *E. coli* have demonstrated that each subunit folds into two distinct N- and C-terminal motifs with the active site positioned in a cleft formed between these domains (*3*−*5*). The N-terminal domain contains seven strands of parallel β-pleated sheet flanked on either side by a total of six α-helices, while the C-terminal domain contains five β-strands and four helical regions. Amino acid sequence analyses have demonstrated that epimerase belongs to a superfamily of proteins referred to as the short-chain dehydrogenases and including such enzymes as mammalian 3β-hydroxysteroid dehydrogenase, plant dihydroflavonol reductase, *Nocardia* cholesterol dehydrogenase, and open reading frames in vaccinia virus and fish lymphocystis disease virus (*6*). In addition, three-dimensional structural comparisons have shown that epimerase, 3α,20β-hydroxysteroid dehydrogenase, and dihydropteridine reductase fold into a common core of approximately 180 equivalent amino acid residues (*7*). All three enzymes contain a Tyr-$(Xaa)_3$-Lys motif thought to be important for their catalytic activities (*5*, *8*−*12*).

According to the presently available biochemical and biophysical data, the reaction mechanism of epimerase is thought to occur through the transient reduction of the NAD^+ cofactor to NADH (*13*). It is believed that the first step in the catalytic mechanism of the enzyme proceeds with the concerted abstraction of the proton from the 4′-hydroxyl group of the UDP-galactose substrate by an active site base and the transfer of the C-4 hydride to NAD^+. The resulting 4′-ketopyranose intermediate presumably rotates in the active site via several torsional angles defined by the phosphate backbone of the uridine nucleotide, thereby presenting the opposite face of the sugar to the NADH. Subsequent oxidation of the NADH and return of the proton to the 4′-keto group result in the product, UDP-glucose. The reaction is readily reversible so that UDP-glucose is converted into UDP-galactose under certain physiological conditions. This nonstereospecificity of epimerase is atypical for enzymes

[†] This research was supported in part by grants from the NIH (DK47814 to H.M.H. and GM15950 to J.B.T.).

[‡] The atomic coordinates have been deposited in the Brookhaven Protein Data Bank under file names 1KVR (S124A·NADH·UDP complex), 1KVQ (S124A·NADH·UDPglucose complex), 1KVS (S124T·NADH·UDPglucose complex), 1KVT and (S124V·NADH·UDPglucose complex).

* To whom correspondence should be addressed.

[⊗] Abstract published in *Advance ACS Abstracts,* August 15, 1997.

S0006-2960(97)00431-5 CCC: $14.00

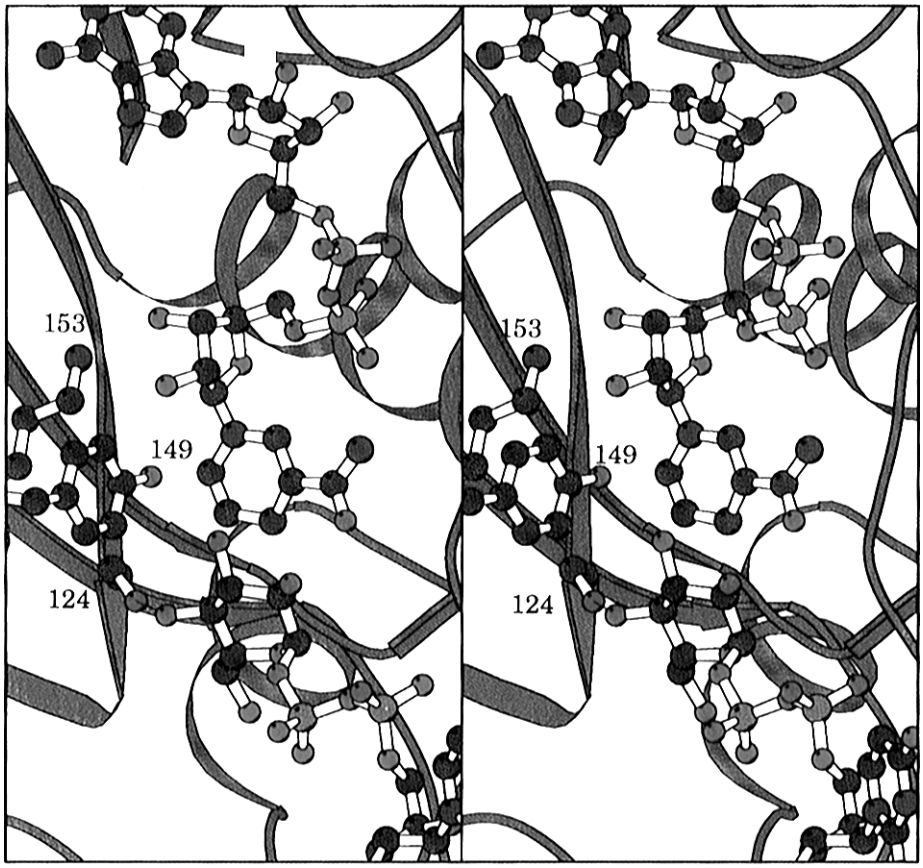

FIGURE 1: Closeup view of the active site of UDP-galactose 4-epimerase complexed with NADH and UDP-glucose. This figure and Figures 3 and 8 were prepared with the software package MOLSCRIPT (*22*). The polypeptide chain backbone is drawn in a ribbon representation, and the nucleotides are depicted as balls and sticks. The "catalytic triad" residues, Ser 124, Tyr 149, and Lys 153, are also displayed in ball and stick representations. The thin bond between O^{γ} of Ser 124 and the 4′-hydroxyl group of the glucose is meant to emphasize the close contact of 2.6 Å observed between these two atoms in the crystalline structure of the abortive complex.

employing NAD^+/NADH cofactors and, indeed, has encouraged much of the current research interest. Until recently, it was believed that a "traditional" base, such as an aspartate, a glutamate, or a histidine, was responsible for proton abstraction. The high-resolution X-ray structure of the epimerase·NADH·UDP-glucose abortive complex by Thoden et al. (*4*) has demonstrated, however, that there are no such residues located in the correct position to serve as the catalytic base. Rather, as shown in Figure 1, O^{γ} of Ser 124 is located 2.6 Å from the 4′-hydroxyl group of the sugar substrate. In an attempt to explore more fully the role of Ser 124 in the epimerase reaction mechanism, three site-directed mutants of the enzyme, namely S124A, S124T, and S124V, have been constructed. The X-ray structures of these mutant proteins are described here and their kinetic parameters discussed in preceding paper (*14*).

MATERIALS AND METHODS

Basic Construction of Plasmids Encoding Mutant Epimerase Genes. The plasmids employed for this investigation were constructed by cassette mutagenesis starting from the pTZSynE plasmid that contained a synthetic gene for the epimerase (*14*). The pTZSynE plasmid was designed with conveniently placed restriction sites located throughout the coding region of the gene. Plasmids containing the site-directed mutants were constructed by ligation of double-stranded DNA cassettes having the appropriate mutations into plasmids from which the wild-type cassettes were removed. All plasmid manipulations were performed with AG-1 bacteria (Stratagene, La Jolla, CA), and plasmids containing the appropriate mutant genes were subsequently transformed into BL21(DE3)pLysS cells (Novagen, Madison, WI) for induction and expression of the protein.

Construction of the Plasmid Containing the S124A Mutation. Since the codon for Ser 124 was located on a restriction site in the synthetic gene, it was necessary to employ an 83-base pair cassette to generate the S124A plasmid. This large cassette was constructed with the following four oligonucleotides, all of which were obtained from Gibco BRL (Grand Island, NY):

(1) Ep1, GGAGCGCGCCGCCAACGTCAAAAACTTTATTTTCTCGAGCGCAGCCACC; (2) Ep2, TGCGCTCGAGAAAATAAAGTTTTTGACGTTGGCGGCGCGCTCC; (3) Ep3, GTTTATGGCGATCAGCCCAAAATTCCATATGAGG; (4) Ep4, CCTCATATGGAATTTTGGGCTGATCGCCATAAACGGTGGC.

These oligonucleotides formed two double-stranded DNA linkers that overlapped by six bases. The four oligonucleotides were boiled for 5 min and then cooled to 4 °C for hybridization into the 83-base pair double-stranded cassette. The cassette was designed to contain a *Bss*HII restriction site at the 5′ end and an *Nde*I restriction site on the 3′ end and to generate a new *Xho*I restriction site adjacent to codon 124 so that subsequent mutations could be more easily constructed. Following hybridization at 4 °C, the double-stranded DNA was treated with T4 DNA ligase (New England Biolabs, Beverly, MA) for 2 h to covalently close the gap between the two oligonucleotides that formed each

Table 1: Intensity Statistics

		resolution range (Å)						
	overall	30.0−4.11	3.26	2.85	2.59	2.41	2.26	2.15
S124A·NADH·UDP-glucose								
no. of measurements	46398	7123	7708	7084	7177	6837	6436	6033
no. of independent reflections	24017	3570	3273	3430	3412	3433	3466	3034
completeness (%)	96	96	91	98	96	95	93	90
average intensity	3429	10000	7012	2899	1490	1053	792	714
average σ	152	262	225	137	109	110	111	116
R factor[a] (%)	3.5	1.8	2.7	4.6	6.5	8.4	9.9	11.0
S124V·NADH·UDP-glucose								
no. of measurements	55317	11380	10270	8721	7735	7061	5944	4206
no. of independent reflections	23699	3574	3490	3458	3436	3417	3433	2980
completeness (%)	96	98	98	99	99	95	92	98
average intensity	5160	10000	8294	4106	2348	1699	1426	1313
average σ	346	330	398	339	323	331	342	358
R factor[a] (%)	4.4	2.8	4.3	6.5	8.9	11.2	12.4	13.8
S124T·NADH·UDP-glucose								
no. of measurements	68358	13923	12369	10659	9584	8617	7592	5614
no. of independent reflections	24177	3702	3552	3545	3535	3449	3392	3002
completeness (%)	95	98	97	99	99	98	90	87
average intensity	5720	10000	9664	4879	3001	2504	2249	2280
average σ	577	345	341	558	595	655	743	893
R factor[a] (%)	6.4	3.6	6.1	9.7	14.2	17.7	21.4	24.5

		resolution range (Å)						
	overall	30.0−3.63	2.88	2.52	2.29	2.13	2.00	1.90
S124A·NADH·UDP								
no. of measurements	59499	11993	8966	9135	8298	7548	7013	6546
no. of independent reflections	32462	4725	4872	4870	4786	4608	5128	4196
completeness (%)	93	90	96	98	96	96	90	85
average intensity	3589	10000	5154	2141	1331	1077	752	518
average σ	240	299	260	209	206	218	228	229
R factor[a] (%)	3.5	2.2	3.7	6.3	8.7	10.3	14.6	19.7

[a] R factor $= (\sum|I - \bar{I}|/\sum I) \times 100$.

strand. Subsequently, the 83-base pair cassette was digested with *Bss*HII and *Nde*I restriction enzymes (New England Biolabs) and purified with the MerMAID DNA purification kit (Bio101, Vista, CA). The wild-type pTZSynE plasmid was digested with the same enzymes, isolated by agarose gel electrophoresis, and purified with the GeneClean DNA purification kit (Bio101). The mutagenic cassette was ligated into the wild-type vector. The sequence surrounding the mutagenic cassette was confirmed by double-stranded DNA sequencing with Sequenase 2.0 (U.S. Biochemicals, Cleveland, OH).

Construction of the Plasmids Containing the S124T and S124V Mutations. The S124T and S124V mutant plasmids were constructed starting with the S124A plasmid. The *Xho*I restriction site adjacent to codon 124 in the S124A plasmid allowed for the use of a shorter mutagenic cassette. The complementary oligonucleotides for S124T listed below were designed to generate a silent *Sca*I restriction site to facilitate identification of mutant plasmids:

(1) S124T-top, TCGAGTACTGCCACCGTTTATGGCGATCAGCCCAAAATTCCA; (2) S124T-bot, TATGGAATTTTGGGCTGATCGCCATAAACGGTGGCAGTAC. Likewise, the complementary oligonucleotides for S124V listed below were designed similarly with a silent *Msc*I restriction site:

(1) S124V-top, TCGAGCGTGGCCACCGTTTATGGCGATCAGCCCAAAATTCCA; (2) S124V-bot, TATGGAATTTTGGGCTGATCGCCATAAACGGTGGCCACGC. The mutagenic cassettes contained overhangs compatible with *Xho*I and *Nde*I restriction sites at the 5′ and 3′ ends, respectively. Each mutagenic cassette was formed by boiling the complementary oligonucleotides and cooling to 4 °C. The cassettes were ligated into the S124A plasmid that was digested with *Xho*I and *Nde*I enzymes and gel-purified with the GeneClean kit. The sequences of the resulting plasmids were confirmed by double-stranded cDNA sequencing of the mutated region.

Purification and Crystallization Procedures. All the above-mentioned site-directed mutant proteins were purified according to previously described methods (*3*). As isolated, the proteins contain tightly bound and mostly oxidized pyridine nucleotide. For the formation of the epimerase S124A, S124T, or S124V·NADH·UDP-glucose abortive complexes, each enzyme sample was treated with a 75 mM dimethylamine−borane complex for 2 h at room temperature as described in ref 4. Solid UDPglucose was subsequently added to each protein sample until a concentration of 15 mM was obtained. These mixtures were incubated for 4 h at room temperature, after which additional dimethylamine−borane complex was added to yield final concentrations of 150 mM. Following incubation at 4 °C for approximately 12 h, the reaction mixtures were dialyzed against 10 mM potassium phosphate (pH 8.0) for 24 h at 4 °C. Each protein sample was subsequently concentrated to 30 mg/mL and additional UDPglucose was added to a final concentration of 10 mM. An analogous method was employed for forming the S124A·NADH·UDP and S124T·NADH·UDP complexes.

Large single crystals for each mutant protein were grown by the hanging drop method of vapor diffusion at 4 °C. The precipitant was typically 14−20% poly(ethylene glycol)

Table 2: Refinement Statistics for the S124A·NADH·UDP Complex

resolution limits (Å)	30.0−1.90
R factor (%)[a]	17.9
no. of reflections used	32 462
no. of protein atoms	2694
no. of solvent atoms	542
weighted root-mean-square deviations from ideality	
bond length (Å)	0.014
bond angle (deg)	2.34
planarity (trigonal) (Å)	.008
planarity (other planes) (Å)	0.010
torsional angle (deg)[b]	14.9

[a] R factor $= \sum|F_o - F_c|/\sum|F_o|$, where F_o is the observed structure-factor amplitude and F_c is the calculated structure-factor amplitude. [b] The torsional angles were not restrained during the refinement.

Table 3: Refinement Statistics for the S124A·NADH·UDP-glucose Complex

resolution limits (Å)	30.0−2.15
R factor (%)[a]	17.3
no. of reflections used	24 017
no. of protein atoms	2715
no. of solvent atoms	482
weighted root-mean-square deviations from ideality	
bond length (Å)	0.015
bond angle (deg)	2.27
planarity (trigonal) (Å)	0.007
planarity (other planes) (Å)	0.013
torsional angle (deg)[b]	15.2

[a] R factor $= \sum|F_o - F_c|/\sum|F_o|$, where F_o is the observed structure-factor amplitude and F_c is the calculated structure-factor amplitude. [b] The torsional angles were not restrained during the refinement.

Table 4: Refinement Statistics for the S124T·NADH·UDP-glucose Complex

resolution limits (Å)	30.0−2.15
R factor (%)[a]	18.8
no. of reflections used	24 177
no. of protein atoms	2706
no. of solvent atoms	426
weighted root-mean-square deviations from ideality	
bond length (Å)	0.015
bond angle (deg)	2.68
planarity (trigonal) (Å)	0.009
planarity (other planes) (Å)	0.014
torsional angle (deg)[b]	16.2

[a] R factor $= \sum|F_o - F_c|/\sum|F_o|$, where F_o is the observed structure-factor amplitude and F_c is the calculated structure-factor amplitude. [b] The torsional angles were not restrained during the refinement.

Table 5: Refinement Statistics for the S124V·NADH·UDP-glucose Complex

resolution limits (Å)	30.0−2.15
R factor (%)[a]	17.8
no. of reflections used	23699
no. of protein atoms	2706
no. of solvent atoms	389
weighted root-mean-square deviations from ideality	
bond length (Å)	0.016
bond angle (deg)	2.57
planarity (trigonal) (Å)	0.006
planarity (other planes) (Å)	0.009
torsional angle (deg)[b]	15.2

[a] R factor $= \sum|F_o - F_c|/\sum|F_o|$, where F_o is the observed structure-factor amplitude and F_c is the calculated structure-factor amplitude. [b] The torsional angles were not restrained during the refinement.

8000, 500−750 mM NaCl, and 50 mM CHES (pH 9.0). Crystal growth was generally complete within 5 days with some crystals achieving maximum dimensions of 0.5 mm × 0.5 mm × 0.5 mm. All of the crystals belonged to the space group $P3_221$ with the typical unit cell dimensions: $a = b = 83.8$ Å, $c = 108.4$ Å, and one subunit per asymmetric unit.

X-ray Data Collection and Processing. Prior to X-ray data collection, the crystals were transferred to cryoprotectant solutions containing 25% poly(ethylene glycol) 8000, 750 mM NaCl, 20% ethylene glycol, and 50 mM CHES (pH 9.0). Each crystal was subsequently suspended in a thin film of the cryoprotectant mixture using a loop composed of fine surgical thread and flash-cooled to −150 °C in a nitrogen stream.

All X-ray data were collected at −150 °C with a Siemens HI-STAR area detector system equipped with double-focusing mirrors. The X-ray source was CuKα radiation from a Rigaku RU200 rotating anode generator operated at 50 kV and 90 mA and equipped with a 300 μm focal cup. Only one crystal was required for each data set.

The X-ray data were processed according to the procedure of Kabsch (*15*, *16*) and internally scaled with the program XCALIBRE (G. Wesenberg and I. Rayment, unpublished results). Relevant X-ray data collection statistics can be found in Table 1.

Computational Methods. The previously determined structure of the epimerase·NADH·UDP-glucose abortive complex, as described in ref 4, served as the starting model for the least-squares refinements of each mutant enzyme with the software package TNT (*17*). The coordinates for Ser 124 and all solvents were deleted from the starting models and rebuilt during the course of the least-squares refinements. Ideal stereochemistries for the NADH and UDP moieties were based on the previously described small molecule structural determinations (*18*−*20*). All manual model building was accomplished with the program FRODO (*21*). Relevant refinement statistics for each model can be found in Tables 2−5.

RESULTS

Description of the S124A·NADH·UDP and the S124A·NADH·UDP-glucose Complexes. The first structure to be solved in this series of site-directed mutants was that of the S124A·NADH·UDP complex. Electron density corresponding to the nucleotides and the polypeptide chain from Ser 122 to Thr 126 is displayed in Figure 2. The model was refined to a nominal resolution of 1.9 Å with an overall *R* factor of 17.9% for all measured X-ray data. In addition to 528 water molecules, an ethylene glycol molecule, a di(ethylene glycol) molecule, and three sodium ions were located in the electron density map. The overall *B* values for the polypeptide chain backbone atoms, the two nucleotides, and the solvents were 19.2, 15.9, and 43.1 Å^2, respectively.

In the wild type·NADH·UDP complex, the nicotinamide ring of the dinucleotide adopts the *anti* conformation with respect to the ribose and the carbonyl oxygen of the carboxamide group is involved in hydrogen bonding interactions with O^{γ} of Ser 124 (2.4 Å) and O^{η} of Tyr 149 (2.7 Å) (*3*). This tight interaction with Ser 124 and Tyr 149 forces the carboxamide group out of the plane of the nicotinamide ring by approximately 25°, thereby disrupting the resonance stabilization of the reduced coenzyme. In the oxidized form

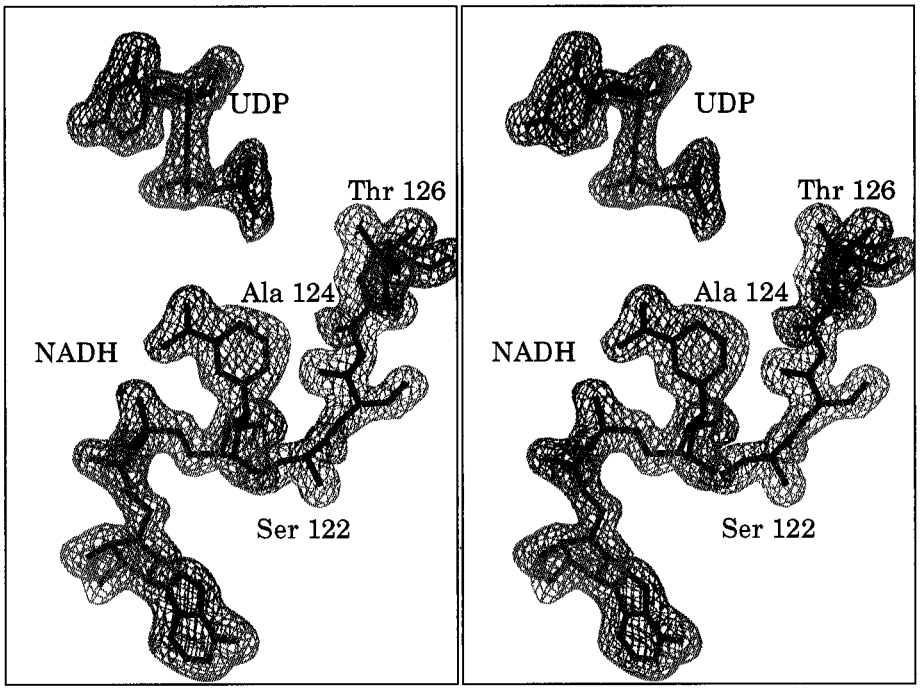

FIGURE 2: Representative electron density for the S124A·NADH·UDP complex. The electron density shown was calculated to 1.9 Å resolution with coefficients of the form $F_o - F_c$, where F_o and F_c were the native and calculated structure-factor amplitudes, respectively. The x-ray coordinates for the nucleotides and for Ser 122−Thr 126 were omitted from the calculation. The map was contoured at 3σ.

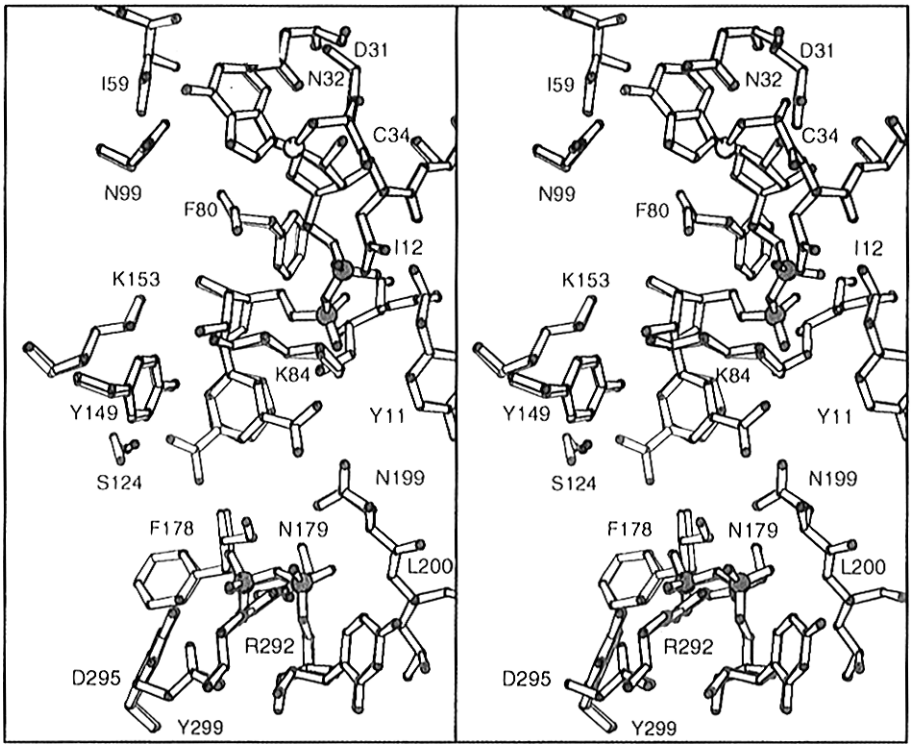

FIGURE 3: Superposition of the active sites for the wild type·NADH·UDP and the S124A·NADH·UDP enzyme complexes. Those amino acid residues that are within approximately 3.2 Å of the dinucleotides are shown. The wild-type structure is depicted in red; the S124A mutant protein model is displayed in black.

of the protein, however, the nicotinamide ring is in the *syn* conformation as would be expected for a *B* side-specific enzyme (*3*). Consequently, the position of the nicotinamide ring in the wild-type protein with bound UDP is dependent upon the redox state of the dinucleotide. As can be seen in Figure 2, however, the nicotinamide ring of the NADH adopts the *syn* conformation in the S124A mutant. Clearly, the hydroxyl group of Ser 124 plays an important structural role in the positioning of the nicotinamide ring. In the wild type·NADH·UDP-glucose abortive complex, where Ser 124 forms a hydrogen bond to the 4′-hydroxyl group of the sugar, the nicotinamide ring is in the *syn* conformation (*4*). In those protein complexes, however, where Ser 124 does not participate in hydrogen bonding to the substrate, its side chain hydroxyl group is free to interact with the carbonyl oxygen of the carboxamide group of NADH, thereby pulling the nicotinamide ring out of the proper position expected for a *B* side-specific enzyme (*4*, *5*). The loss of a hydroxyl group

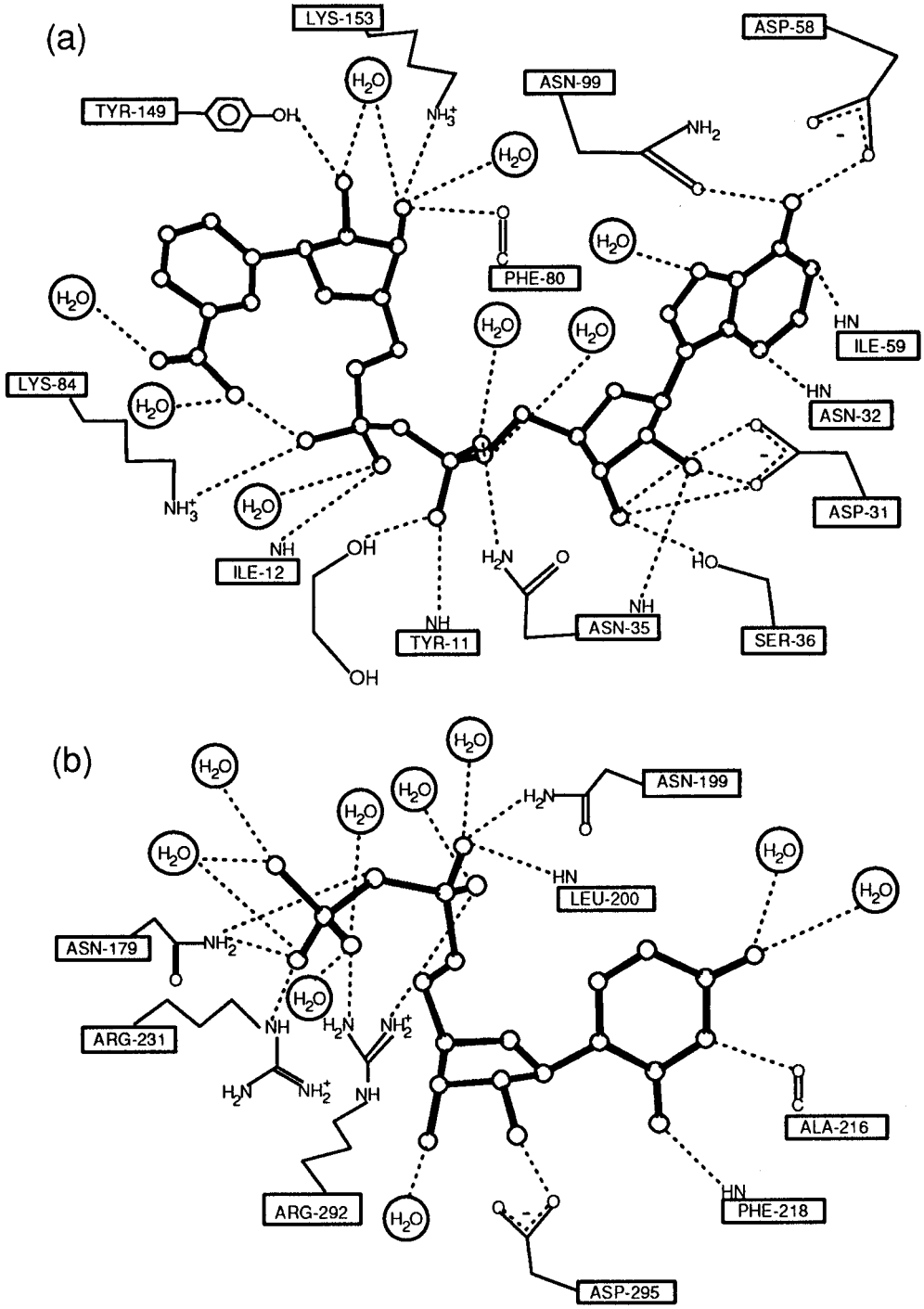

FIGURE 4: Schematic representation of the hydrogen bonding pattern surrounding the nucleotides in the S124A mutant enzyme complex. Those possible hydrogen bonds within 3.2 Å between the protein and (a) NADH and (b) UDP are indicated by the dashed lines.

in the S124A enzyme results in the nicotinamide moiety adopting the proper *syn* conformation and the carboxamide group lying approximately in the plane of the nicotinamide ring.

A superposition of the active site regions for the wild type·NADH·UDP and S124A·NADH·UDP models is given in Figure 3. As can be seen, there are minimal changes in the two structures apart from the position of the nicotinamide rings which are related to one another by an approximate 160° rotation about the glycosidic bonds. All main chain atoms for the two models were superimposed with a root-mean-square deviation of 0.14 Å. Potential hydrogen bonds between the NADH and the S124A protein are schematically shown in Figure 4a. Those interactions observed between the diphosphate and adenine portions of the NADH and the protein are virtually identical in the wild-type and S124A mutant enzymes. The only significant differences occur at the nicotinamide portion of the NADH where the interactions between the dinucleotide and the S124A mutant protein resemble those observed for the wild type·NAD^+·UDP enzyme complex (*3*). The interactions between the protein and the UDP, as depicted in Figure 4b, are again basically identical to those observed in the wild type·NADH·UDP structure (*3*).

In an effort to more fully address the role of position 124 in the biochemical activity of epimerase, the second structure to be studied in this investigation was that of the S124A·NADH·UDP-glucose complex. The structure was refined to

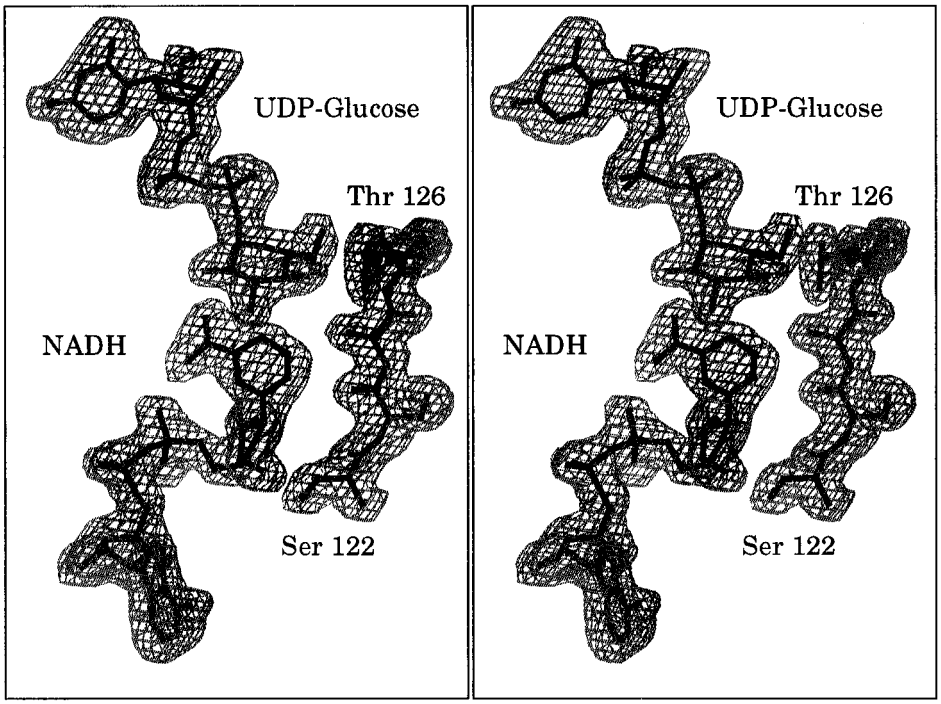

FIGURE 5: Representative electron density for the S124A·NADH·UDP-glucose complex. The electron density shown was calculated and contoured as described in Figure 2.

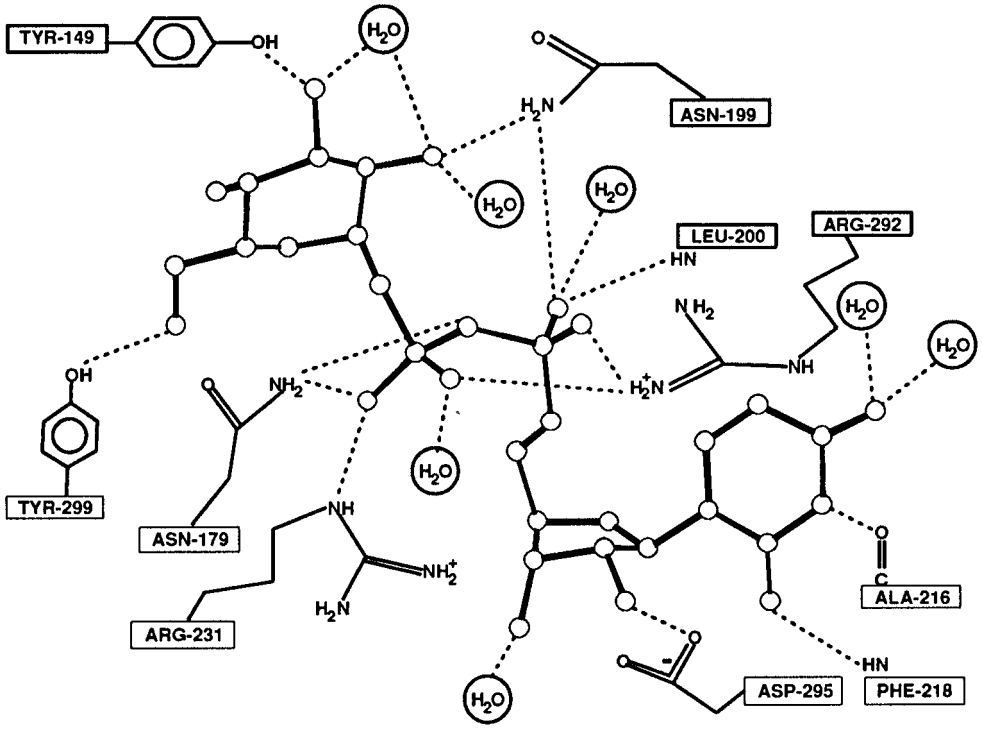

FIGURE 6: Observed hydrogen bonding pattern between the S124A mutant protein and the UDP-glucose. The dashed lines indicate possible hydrogen bonds within 3.2 Å.

a nominal resolution of 2.15 Å with an overall *R* value of 17.3% for all measured X-ray data. In addition to 476 water molecules, one ethylene glycol moiety and two sodium ions were also included in the final model. Representative electron density for the region surrounding the mutation is shown in Figure 5. As can be seen, the electron density corresponding to the glucose is well-ordered and unambiguous. All polypeptide chain backbone atoms for the wild type·NADH·UDP-glucose and S124A·NADH·UDP-glucose structures were superimposed with a root-mean-square deviation of 0.14 Å. In addition, the NADH and UDP-glucose moieties correspond with a root-mean-square deviation of 0.16 Å. The hydrogen bonding pattern between the protein and the UDP-glucose substrate, as shown schematically in Figure 6, is the same as that observed for the wild-type enzyme abortive complex with the one exception being the loss of the O^{γ} (Ser 124) to 4′-hydroxyl (UDP-glucose) electrostatic interaction. The β-carbon of Ala 124 is located 3.5 Å from the 4′-hydroxyl group of the substrate. As described in ref 14 there is a significant loss of catalytic

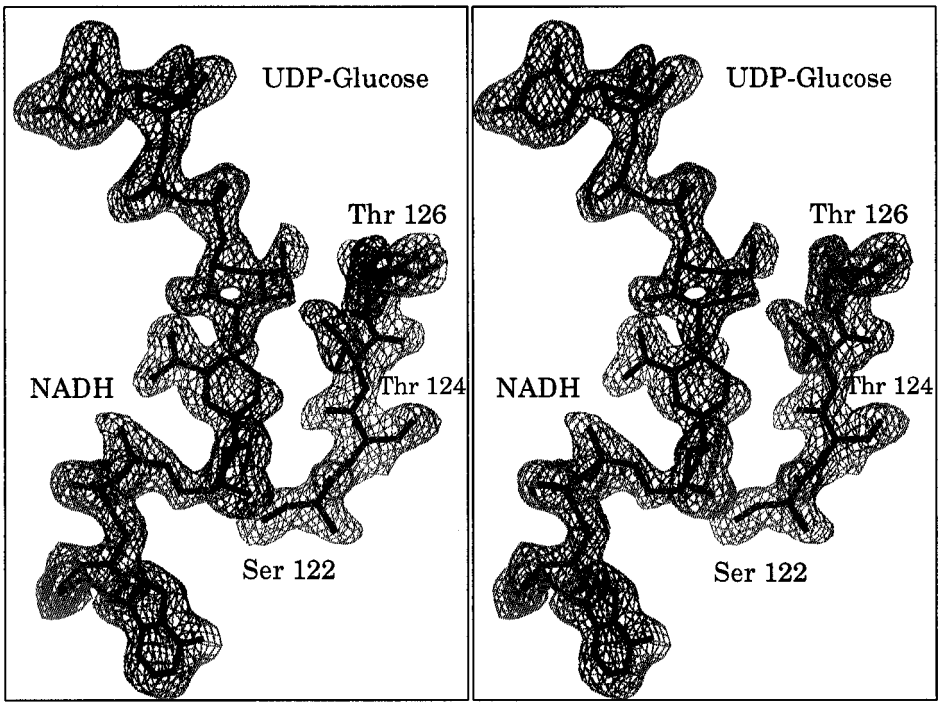

FIGURE 7: Representative electron density for the T124A·NADH·UDP-glucose complex. The electron density shown was calculated and contoured as described in Figure 2.

activity when Ser 124 is replaced by an alanine. The results described here clearly indicate that this loss of enzymatic function is not due to major structural changes in the active site but rather to the loss of a hydroxyl group at position 124.

Description of the S124T·NADH·UDP-glucose Complex. To further explore the structural role of a hydroxyl group at position 124, the next site-directed mutant to be constructed in this study was that in which Ser 124 was replaced with a threonine. This mutant protein did, indeed, demonstrate catalytic activity, albeit at a reduced level (*14*). The structure of the S124T·NADH·UDP-glucose complex described here was refined to a nominal resolution of 2.15 Å with a crystallographic *R* factor of 18.8%. The final model included 417 water molecules, one di(ethylene glycol) moiety, and two sodium ions. Average *B* values for the polypeptide chain backbones atoms, the nucleotides, and the solvent molecules were 30.3, 28.0, 44.1 Å^2, respectively.

Electron density corresponding to the region of the mutation is shown in Figure 7. It was anticipated that O$^{\gamma}$ of Thr 124 would project toward the 4′-hydroxyl group of the glucose and as such was initially modeled into the electron density map in this conformation. However, repeated cycles of least-squares refinement and manual model building indicated that the better fit to the electron density map involved a torsional rotation of approximately 120° about the Cα−Cβ bond thereby orienting C$^{\gamma}$ rather than O$^{\gamma}$ toward the sugar hydroxyl. In this conformation, C$^{\gamma}$ is located 2.8 Å from the 4′-hydroxyl group of glucose.

A superposition of the active sites for the wild type·NADH·UDP-glucose and the S124T·NADH·UDP-glucose complexes is displayed in Figure 8. The main chain backbone atoms for these two models correspond with a root-mean-square deviation of 0.19 Å, while the nucleotides superimpose with a root-mean-square deviation of 0.30 Å. As in the S124A mutant complexes, there are minimal changes in the active sites between the native and S124T proteins. The hydrogen bonding pattern surrounding the UDPglucose substrate in the S124T enzyme is basically identical to that observed in the S124A abortive complex except for slight variations in the water structure surrounding the uridine ring.

The importance of a hydroxyl group at position 124 in stabilizing the *anti* conformation of the nicotinamide ring of NADH was further investigating by determining the structure of the S124T·NADH·UDP complex. It was anticipated that the nicotinamide ring would adopt the *anti* conformation. X-ray data were collected to 2.7 Å, and the resulting electron density map clearly indicated, however, that the nicotinamide ring was in the *syn* conformation as observed in the wild type·NAD$^+$·UDP protein (J. B. Thoden, unpublished results). In retrospect, the observed *syn* conformation is not surprising given the steric hindrance imposed by the presence of an additional methyl group on the threonine. It is not possible to spatially accommodate both a threonine residue at position 124 and the *anti* conformation of the nicotinamide ring since this would lead to atom−atom contacts closer than 1.4 Å.

Description of the S124V·NADH·UDP-glucose Complex. The final site-directed mutant protein to be constructed for this investigation had Ser 124 replaced with a valine. Again, the structure was refined to a nominal resolution of 2.15 Å with an overall crystallographic *R* value of 17.8%. In addition to 381 water molecules, the model contained one di(ethylene glycol) moiety and one sodium ion. Of the three site-directed mutant proteins described here, the catalytic activity is the most reduced for the S124V enzyme (*14*). Electron density corresponding to the region surrounding the mutation is depicted in Figure 9. While the polypeptide chain is well-ordered with an average *B* value of 26.7 Å^2, the electron density for the glucose molecule is weak, thus indicating possible multiple conformations. The average

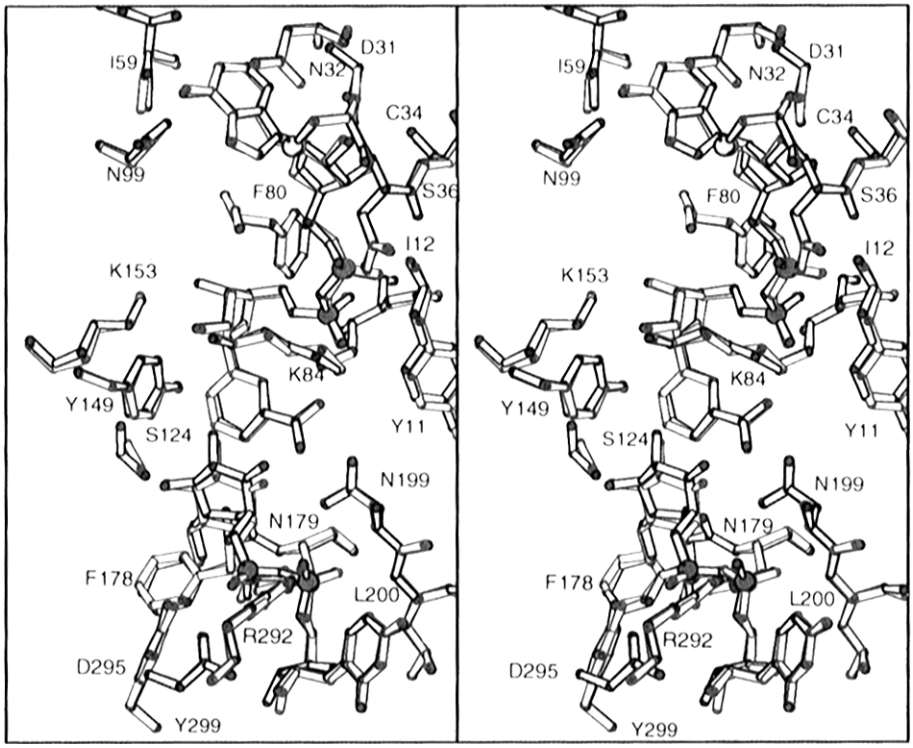

FIGURE 8: Superposition of the active sites for the wild type·NADH·UDP-glucose and the S124T·NADH·UDP-glucose complexes. The wild-type and mutant proteins are displayed in red and black, respectively.

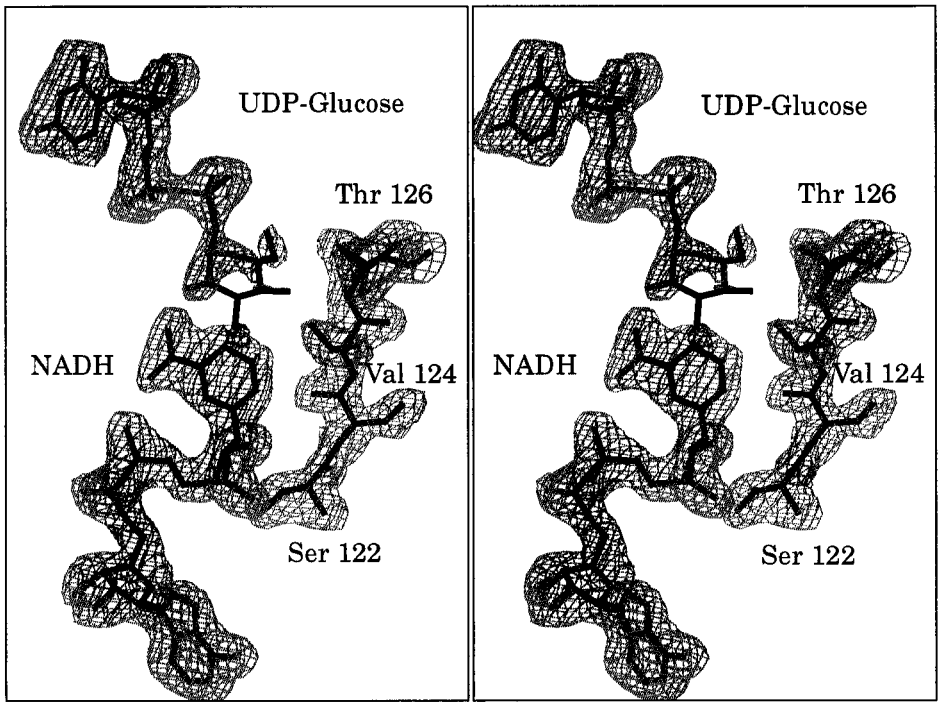

FIGURE 9: Representative electron density for the S124V·NADH·UDP-glucose complex. The electron density shown was calculated and contoured as described in Figure 2.

temperature factor for the glucose moiety in the S124V protein is 59 Å^2. For comparison, the average *B* values for the glucose moieties in the S124A and S124T enzyme complexes were 43 and 49 Å^2, respectively. The lack of a hydroxyl group at position 124 may allow for alternate conformations of the sugar. Note that, for the S124V protein, the valine adopts the staggered orientation opposite to that observed for the threonine mutation. In the model depicted in Figure 9, C$^{\gamma 2}$ of Val 124 lies 2.5 Å from the 4′-hydroxyl group of the UDP-glucose. The hydrogen bonding pattern around the substrate in the S124V abortive complex is depicted in Figure 10. As can be seen by comparing it with Figure 6, there are several slight variations in the hydrogen bonding patterns observed for the substrates in the S124A and S124V mutant enzymes. In particular, one of the carboxylate oxygens of Asp 295 is located 2.8 Å from the 2′-hydroxyl of the uridine ribose in the S124A protein, while in the S124V enzyme, it is positioned at 3.3 Å. Also, there is an additional water molecule near the guanidinium group of Arg 292 in the S124V protein which hydrogen bonds to

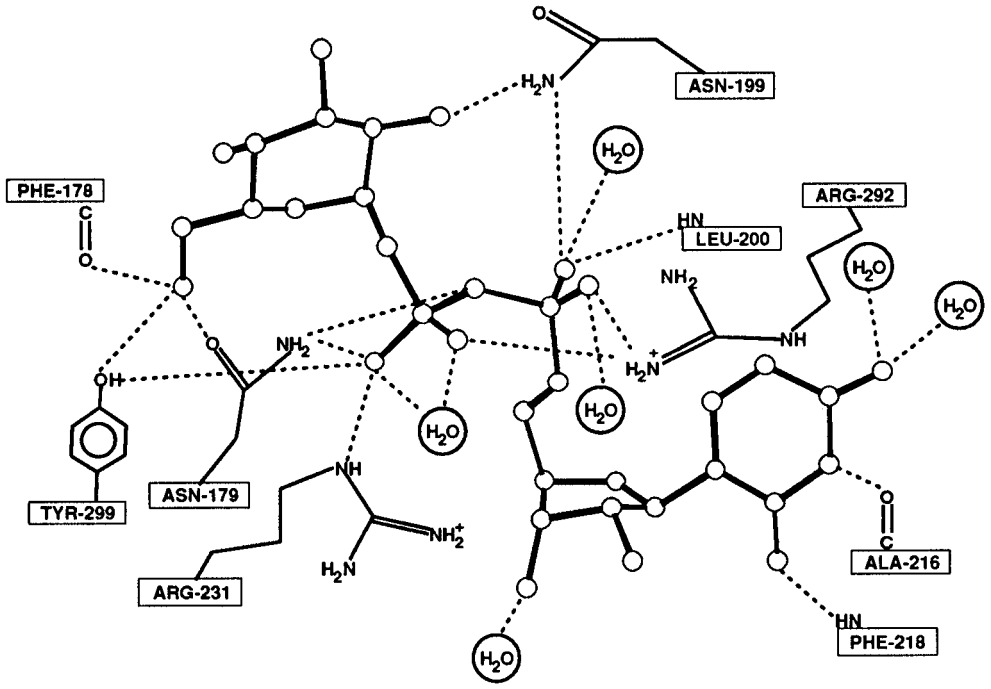

FIGURE 10: Observed hydrogen bonding pattern between the S124V mutant protein and the UDP-glucose. The dashed lines indicate possible hydrogen bonds within 3.2 Å.

one of the phosphoryl oxygens of the UDP moiety. This solvent is absent in the S124A enzyme. The most significant differences occur near the sugar group. While O^{η} of Tyr 149 hydrogen bonds to the 3′-hydroxyl of glucose in the S124A protein, it is located 3.5 Å from the 3′-hydroxyl in the S124V molecule. There are two additional water molecules positioned within 3.2 Å of the glucose in the S124A but not in the S124V protein as shown in Figures 6 and 10. One final difference occurs with respect to the carbonyl oxygen of Phe 178. In the S124V and S124A proteins, the distances between the carbonyl oxygens of Phe 178 and the C-6 hydroxyl groups of the sugars are 2.9 and 3.5 Å, respectively. All backbone atoms for the wild type•NADH•UDP-glucose and the S124V•NADH•UDP-glucose complexes were superimposed with a root-mean-square deviation of 0.17 Å, thus indicating that the loss of catalytic activity for the S124V mutant enzyme is not due to extensive structural perturbations but rather to the absence of a hydroxyl group.

DISCUSSION

Research interest in epimerase has focused recently on several unique features of the enzyme, including the nonstereospecificity of hydride return from the *B* side of the nicotinamide ring of NADH to the 4-ketopyranose intermediate, the conformational flipping of the nicotinamide ring, and the lack of a traditional base within the active site. The nonstereospecificity of hydride return is thought to occur by rotation of the 4-ketopyranose intermediate, and indeed, recent structural studies of epimerase complexed with UDP-mannose, UDP-4-deoxy-4-fluoro-α-D-galactose, or UDP-4-deoxy-4-fluoro-α-D-glucose have suggested that the active site region is large enough to accommodate such a rotation (*23*).

Perhaps one of the more intriguing structural aspects of epimerase, however, is the conformational flipping observed for the nicotinamide ring of the NAD(H). Most NAD^+-dependent enzymes show either the *anti* or *syn* conformation exclusively depending upon whether they are *A* or *B* side-specific. Indeed, since it was known that epimerase is a *B* side-specific enzyme, it was anticipated that the nicotinamide ring would adopt the *syn* conformation with respect to the ribose. Quite surprisingly, the first structure of epimerase, complexed with UDP-phenol, showed the nicotinamide ring positioned in the *anti* conformation (*24*). Subsequent studies of the epimerase•NAD^+•UDP and epimerase•NADH•UDP complexes revealed that the orientation of the nicotinamide ring was dependent upon the redox state of the dinucleotide with the oxidized and reduced forms adopting the *syn* and *anti* conformations, respectively. In addition, the *anti* conformation was stabilized by a hydrogen bond (2.4 Å) between the oxygen of the carboxamide group of the cofactor and O^{γ} of Ser 124 (*3*). The next structural investigation, namely that of the epimerase•NADH•UDP-glucose abortive complex, was especially revealing in that the nicotinamide ring, even though in the reduced state, adopted the *syn* orientation, thereby projecting the *si* face of the nicotinamide ring toward the glycosyl moiety of the substrate (*4*). This study clearly emphasized that the active conformation of the nicotinamide moiety must be *syn* and that the hydrogen bonding capacity of the hydroxyl group at position 124 was satisfied by interaction with the 4′-hydroxyl group of the glucose rather than with the carboxamide group of the dinucleotide (*4*). Additional investigations have now revealed that the nicotinamide ring is in the *syn* orientation in thecomplexesofepimerase•NADH•UDP-mannose,epimerase•NADH•UDP-4-deoxy-4-fluoro-α-D-galactose, and epimerase•NADH•UDP-4-deoxy-4-fluoro-α-D-glucose (*23*). The three-dimensional structures described here once again demonstrate and emphasize the hydrogen bonding potential of a hydroxyl group at position 124 in stabilizing the *anti* conformation of the nicotinamide ring. When this hydroxyl group is removed, as in the case of the S124A mutant protein, the nicotinamide ring adopts the *syn* orientation.

From the present study, it is absolutely clear that the decrease in catalytic activity resulting from the replacement of Ser 124 with an alanine or valine is due to the loss of a properly positioned hydroxyl group and not to major structural perturbations. Indeed, the polypeptide chains for all of the mutant proteins·NADH·UDP-glucose complexes are remarkably similar and can be superimposed onto that of the native enzyme with root-mean-square deviations of not greater than 0.19 Å. Furthermore, on the basis of the results from this study and those described in ref 14, it can be concluded that Ser 124 and Tyr 149 play major functional roles in the reaction mechanism of epimerase and together may provide the required "catalytic" base. That is, in a productive enzyme·NAD^+·UDP-sugar complex, Tyr 149 is ionized but hydrogen-bonded to Ser 124, which in turn forms a hydrogen bond with the 4′-hydroxyl group of the sugar. As hydride transfer occurs from C-4 of the sugar to NAD^+, a double proton shift takes place, leaving the 4′-hydroxyl group oxidized to a ketone, and both Ser 124 and Tyr 149 protonated. Thus, Ser 124 acts as a proton conduit to Tyr 149, which because of its lower pK_a, is the ultimate proton acceptor.

REFERENCES

1. Wilson, D. B., and Hogness, D. S. (1969) *J. Biol. Chem. 244*, 2132−2136.
2. Lemaire, H.-G., and Müller-Hill, B. (1986) *Nucleic Acids Res. 14*, 7705−7711.
3. Thoden, J. B., Frey, P. A., and Holden, H. M. (1996) *Biochemistry 35*, 2557−2566.
4. Thoden, J. B., Frey, P. A., and Holden, H. M. (1996) *Biochemistry 35*, 5137−5144.
5. Thoden, J. B., Frey, P. A., and Holden, H. M. (1996) *Protein Sci. 5*, 2149−161.
6. Baker, M. E., and Blasco, R. (1992) *FEBS Lett. 301*, 89−93.
7. Holm, L., Sander, C., and Murzin, A. (1994) *Struct. Biol. 1*, 146−147.
8. Varughese, K. I., Skinner, M. M., Whiteley, J. M., Matthews, D. A., and Xuong, N. H. (1992) *Proc. Natl. Acad. Sci. U.S.A. 89*, 6080−6084.
9. Varughese, K. I., Xuong, N. H., Kiefer, P. M., Matthews, D. A., and Whiteley, J. M. (1994) *Proc. Natl. Acad. Sci. U.S.A. 91*, 5582−5586.
10. Ghosh, D., Weeks, C. M., Grochulski, P., Duax, W. L., Erman, M., Rimsay, R. L., and Orr, J. C. (1991) *Proc. Natl. Acad. Sci. USA 88*, 10064−10068.
11. Ghosh, D., Wawrzak, Z., Weeks, C. M., Duax, W. L., and Erman, M. (1994) *Structure 2*, 629−640.
12. Ghosh, D., Erman, M., Wawrzak, Z., Duax, W. L., and Pangborn, W. (1994) *Structure 2*, 973−980.
13. Frey, P. A. (1987) in *Pyridine Nucleotide Coenzymes: Chemical, Biochemical, and Medical Aspects* (Dolphin, D., Poulson, R., & Avramovic, O., Eds.) pp 461−511, John Wiley & Sons, Inc., New York.
14. Liu, Y., Thoden, J. B., Berger, E., Kim, J., Swanson, B. A., Gulick, A. M., Ruzicka, F. J., Holden, H. M., and Frey, P. A. (1997) *Biochemistry 36*, 10675−10684.
15. Kabsch, W. (1988) *J. Appl. Crystallogr. 21*, 67−71.
16. Kabsch, W. (1988) *J. Appl. Crystallogr. 21*, 916−924.
17. Tronrud, D. E., Ten Eyck, L. F., and Mathews, B. W. (1987) *Acta Crystallogr. A 43*, 489−501.
18. Reddy, B. S., Saenger, W., Mühlegger, K., and Weimann, G. (1981) *J. Am. Chem. Soc. 103*, 907−914.
19. Viswamitra, M. A., Post, M. L., and Kennard, O. (1979) *Acta Crystallogr. B 35*, 1089−1094.
20. Glasfeld, A., Zbinden, P., Dobler, M., Benner, S. A., and Dunitz, J. D. (1988) *J. Am. Chem. Soc. 110*, 5152−5157.
21. Jones, T. A. (1985) *Methods Enzymol. 115*, 157−171.
22. Kraulis, P. J. (1991) *J. Appl. Crystallogr. 24*, 946−950.
23. Thoden, J. B., Hegeman, A. D., Wesenberg, G., Chapeau, M. C., Frey, P. A., and Holden, H. M. (1997) *Biochemistry* (in press).
24. Bauer, A. J., Rayment, I., Frey, P. A., and Holden, H. M. (1992) *Proteins: Struct., Funct. Genet. 12*, 372−381.

BI9704313